Asociación Argentina
de Mecánica Computacional

Mecánica Computacional Vol XXXVII, págs. 1625-1633 (artículo completo)
A. Cardona, L. Garelli, J.M. Gimenez, P.A. Kler, S. Márquez Damián, M.A. Storti (Eds.)
Santa Fe, 5-7 Noviembre 2019

# NUMERICAL ANALYSIS OF THE CIRCUMFERENTIAL ABLATION OF THE DUODENAL WALL FOR TREATMENT OF TYPE 2 DIABETES

**Bruna R. Loiola[a], Francesco S. Neto[a] and Rodrigo O. C. Guedes[a]**

[a]*Seção de Engenharia Mecânica, Instituto Militar de Engenharia, Praça General Tibúrcio 80, Rio de Janeiro, RJ 22290-270, Brasil, bruna.loiola@ime.eb.br, http://www.ime.eb.br*

**Keywords:** numerical analysis, duodenal resurfacing treatment, Type 2 diabetes.

**Abstract**. This work presents a numerical analysis of the circumferential ablation problem of the duodenum wall for treatment of Type 2 diabetes. Recently, in the literature, an alternative treatment for Type 2 diabetes control has been reported. In this procedure, an endoscopic catheter is inserted into the duodenum through a balloon filled with a hot fluid that allows for a controlled thermal procedure. Experimental results indicate that the damaged layer induces a regulation of hyperglycemia at least for a certain amount of time. Therefore, the objective of this work is to numerically simulate this treatment considering the bioheat transfer equation in the transient form. The finite volume method is used in the discretization of the energy equation and the results are verified by exploring the same problem in a commercial finite-element package. A Dirichlet boundary condition is adopted at the inner surface while a Neumann restriction is considered at the outer surface of the duodenum. The Arrhenius criterion for the evaluation of the thermally affected tissue is employed in this study. According to the simulations, this treatment can produce an irreversible thermal injury of at least 0.7 mm and up to 1.3 mm depending on the blood perfusion rate. The results here advanced suggest the region of the duodenum capable of producing new cells after the therapy is found to be between 2.0 to 3.1 mm depending on the estimate of the blood perfusion rate.

## 1 INTRODUCTION

In current days, Type 2 diabetes has become a major issue concerning health care as it affects millions of people and researchers are involved in developing more efficient treatments. Due to the fact that the absorption of nutrients is performed in the small intestine, therapies targeting the duodenum, jejunum and ileum are of great interest. The lining of duodenum has hormone producing cells whose task is to detect the presence of glucose thus sending a signal to the pancreas to produce insulin. These cells, in patients with Type 2 diabetes, do not act properly and promising new procedures like the recently advanced Duodenal Mucosal Resurfacing (DMR) (Rajagopalan et al. 2016, Hadefi et al. 2018) were devised to deal with this condition. Basically, this treatment performs a thermal ablation at the mucosal surface of the duodenum in which the heat destroys the abnormal cells allowing for the emergence of new healthy ones enabling the human body to produce adequate levels of insulin. Studies like those of Rajagopalan et al. (2016), indicate that after this treatment, significant improvements were observed in glycemic control in human subjects. As this therapy is still under scrutiny, it is believed that a temperature distribution could be of use to further understand the various phenomena involved. Therefore, the main purpose of this contribution deals with the numerical thermal analysis of the Duodenal Mucosal Resurfacing treatment.

## 2 MATHEMATICAL FORMULATION FOR THE DUODENAL MUCOSAL RESURFACING TREATMENT

The duodenal mucosal wall resurfacing consists of a process in which an endoscopic catheter is inserted into the duodenum through an oral mechanism. This probe has a balloon containing hot water at approximately 86 ºC. The procedure has a duration of 10 seconds and it is performed at five distinct parts of duodenum (Hadefi et al. 2018). The heat transfer between the hot water and the mucosal surface destroys the damaged cells allowing for the growth of new ones leading to a better control in insulin body levels. In Frøkjær et al. (2006), a careful description of the duodenum geometry is found. Nonetheless, in this contribution, the duodenal wall is taken as an annular region and the heat transfer problem is described by Pennes' formulation (Pennes, 1948) through a transient, one-dimensional analysis as outlined in Eq. (1). The thermal conductivity related to the tissue is temperature dependent as suggested in Valvano (2011) and Valvano (2018). As described in Eq. (2), the duodenum is assumed to have a uniform body temperature ($T_b$) at the beginning of treatment. The inner surface ($r_i$) is believed to be in perfect thermal contact with the balloon, Eq. (3) while the outer surface ($r_o$) is supposed to be adiabatic in order to simulate the condition associated to a higher probability of thermal damage at the tissue, Eq. (4).

$$C\frac{\partial T(r,t)}{\partial t} = \frac{1}{r}\frac{\partial}{\partial r}\left[k(T)r\frac{\partial T}{\partial r}\right] + \rho_b c_b \omega_b [T_b - T(r,t)] + \dot{Q}_m \qquad r_i < r < r_o \qquad t > 0 \tag{1}$$

$$T(r,t) = T_b \qquad r_i \le r \le r_o \qquad t = 0 \tag{2}$$

$$T(r,t) = T_{balloon} \qquad r = r_i \qquad t > 0 \tag{3}$$

$$\frac{\partial T(r,t)}{\partial r} = 0 \qquad r = r_o \qquad t > 0 \tag{4}$$

In these equations, $C$ indicates the volumetric heat capacity and $k(T)$, the temperature dependent thermal conductivity. The radial direction is represented by $r$, the temperature distribution by $T(r,t)$ and $t$ being the elapsed time of the treatment. The Pennes formulation allows for a metabolic heat source ($\dot{Q}_m$) for the duodenum and lastly, the perfusion term is associated to the blood density ($\rho_b$), blood specific heat capacity ($c_b$) and blood perfusion ($\omega_b$). Generally speaking, both the thermal conductivity and the thermal diffusivity of biological tissues are known to be temperature dependent. Consistent with previous studies, the volumetric heat capacity is taken as constant while a linear fit, as expressed in Eq. (5), describes the behavior of the duodenum thermal conductivity.

$$k(T) = k_0 + k_1 T \tag{5}$$

In this work, the Arrhenius formulation indicated in Eq. (6) is applied to evaluate the thermal injury ($\Omega$) that represents a cumulative damage to the biological tissue. In this particular equation, $A$ represents the scale factor, $R$ is the universal gas constant and $E_a$ is the activation energy. In burn studies (Henriques, 1947; Henriques and Moritz, 1947; Moritz, 1947; Moritz and Henriques, 1947; Thomsen and Pearce, 2011; Pearce, 2013; Wright, 2015; Abraham et al. 2016; Abraham et al. 2018), a value of $\Omega = 1$ is associated to a second-degree burn, i.e. irreversible damage where the existing cells are damaged. For living tissues, this leads to the recuperation of the region and emergence of new cells. In this work, a value of thermal injury above the unity ($\Omega \geq 1$) is used to define the affected area with irreversible damage while the situation involving $\Omega < 1$ represents the affected extension of the duodenum capable of regeneration.

$$\Omega = \int_0^t A e^{\left[-\frac{E_a}{RT}\right]} dt' \tag{6}$$

## 3 CODE AND SOLUTION VERIFICATION

In the absence of solid experimental data, in this section we establish a comparison between a numerical code especially written for this research and a scientific simulation software. The comparison was performed by following the ASME Standard Verification and Validation (2009).

In order to solve the mathematical formulation described in Eq. (1) together with restrictions (2) to (4), a finite volume method (Patankar, 1980; Ozisik et al. 2017) was implemented at a MATLAB® platform using an implicit method. As already mentioned before, the duodenal wall represented in a cylindrical geometry, was considered to have a thickness of 5 mm with an inner radius of 22.5 mm from the center. The verification of the solution was performed by considering three sets of uniform grids having 1000, 1500 and 2250 volumes, respectively, with a time-step of 0.01 s up to a final time of 10 s which is the typical duration of the treatment. The maximum absolute error among the grids was found to be $1.46 \times 10^{-5}$ °C, yielding a relative error of $2.6 \times 10^{-5}$ %. Consequently, the mesh with 1000 volumes was chosen to perform the simulations described in this contribution.

The code verification was established by utilizing the software COMSOL *Multiphysics*®

for comparison purposes. As an initial remark, the physical parameters needed in the simulations together with its references are found in Table 1. The finite element solution was obtained by means of a 2-D axisymmetric model with an extremely refined mesh (2606 triangular elements). Figure 1 presents the spatial temperature distribution at the end of the therapy ($t$ = 10 s) while Figure 2 depicts a comparison between the two numerical methods for the same time. A closer investigation of these values suggests that the maximum relative error between the two numerical simulations is less than 2%.

| Parameter | Value | Unit | Reference |
|---|---|---|---|
| $k_0$ | 0.4365 | W $m^{-1}$ $°C^{-1}$ | Valvano (2018) |
| $k_1$ | 0.002844 | W $m^{-1}$ $°C^{-2}$ | Valvano (2018) |
| $C$ | 3138.030 | kJ $m^{-3}$ $K^{-1}$ | Valvano (2018) |
| $\omega_b$ | 0.0005 | $m_b^3$ $s^{-1}$ $m_t^{-3}$ | Zhao et al. (2018) |
| $c_b$ | 3600 | J $kg^{-1}$ $K^{-1}$ | Zhao et al. (2018) |
| $\rho_b$ | 1000 | kg $m^{-3}$ | Zhao et al. (2018) |
| $\dot{Q}_m$ | 4200 | W $m^{-3}$ | Zhao et al. (2018) |
| $T_b$ | 37 | °C | Zhao et al. (2018) |
| $T_{balloon}$ | 86 | °C | Hadefi et al. (2018) |

Table 1: Parameter values employed in the simulations.

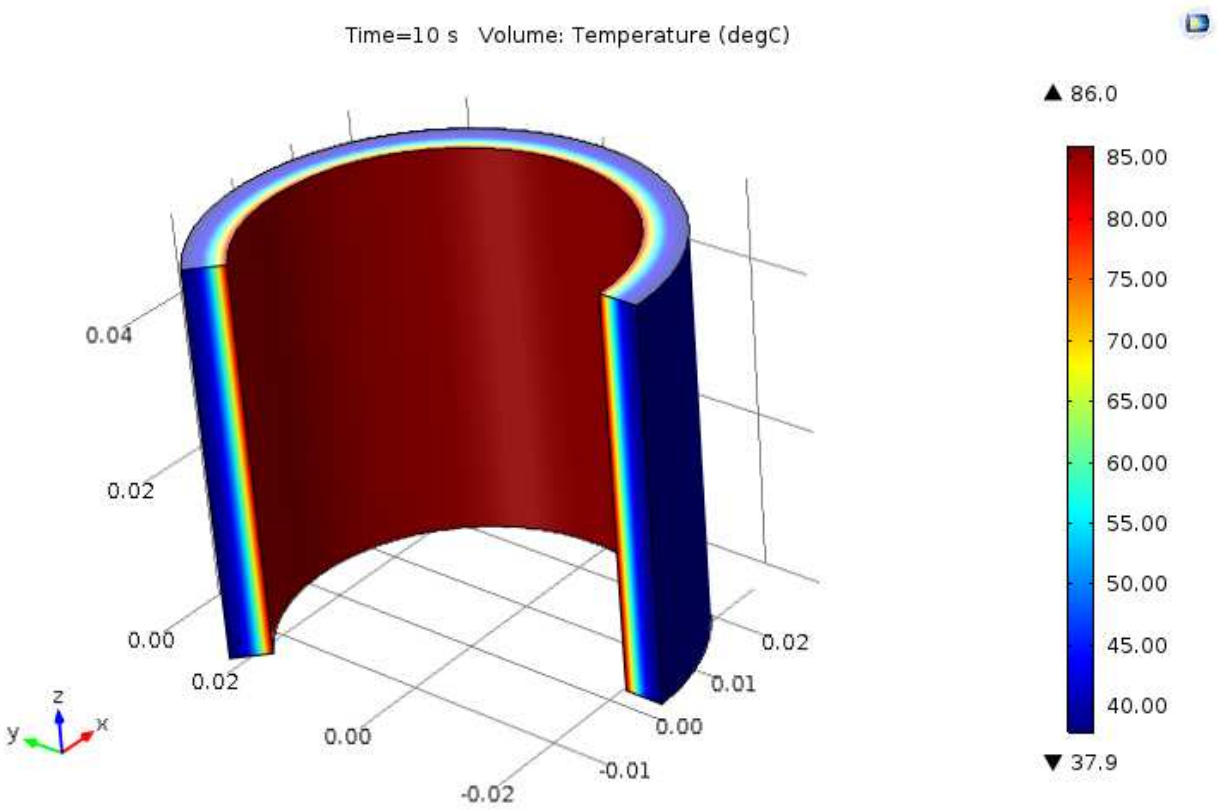


Figure 1: Temperature profile obtained through COMSOL *Multiphysics*® where the dimensions are in meters and the temperature in degree Celsius.

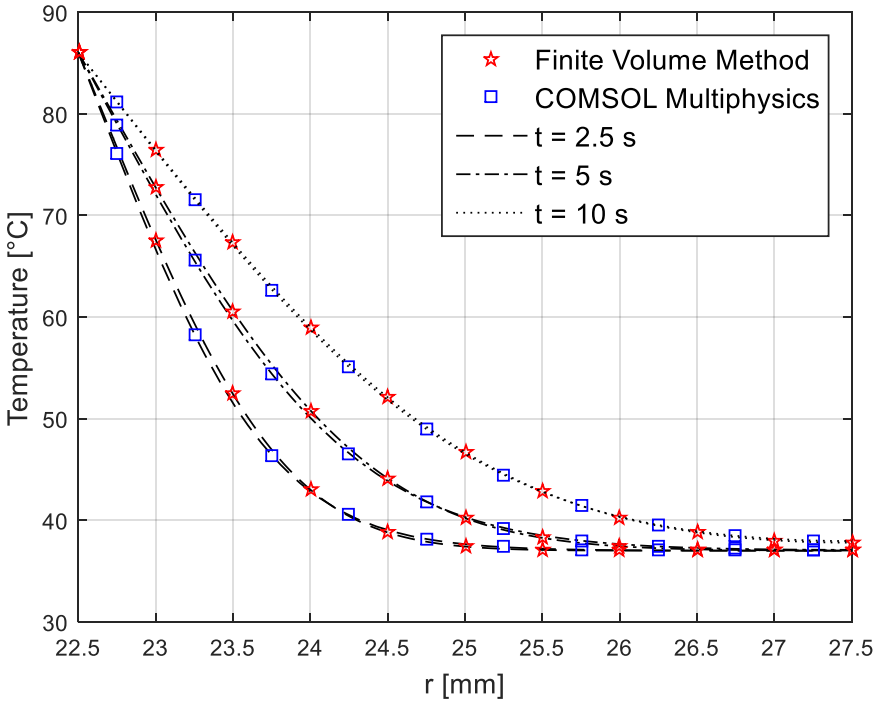


Figure 2: Comparison of the two numerical methods for the radial temperature distribution.

## 4 RESULTS AND DISCUSSION

Temperature distributions and the related evaluation of the Henriques burn integral, Eq. (6), were investigated for the 1000 volume mesh for typical values reported in Table 1 and for all the four cases of the perfusion coefficient displayed in Table 2. Even though the case 2 scenario is the standard value of the perfusion coefficient of biological tissues as suggested by Zhao et al. (2018), further considerations must be taken into account in order to have a more complete insight of the problem at hand. For example, it is a well-known fact that as the temperature of any living tissue increases, the blood perfusion experiences an elevation due to the metabolic activity (Rossmann and Haemmerich, 2014). Furthermore, as the thermal damage progresses, the perfusion rate diminishes up to a point of a null value due to the complete coagulation of the tissue. In order to simulate this particular aspect, the four cases of Table 2 were devised. Figure 3 explores the radial temperature distribution at the end of the 10 s treatment for the four reported cases of the perfusion coefficient and an inspection of these results reveal some interesting trends. Initially, it can be noted that there is no apparent change in the temperature field for the normal perfusion coefficient ($\omega_b = 0.0005\ m_b^3\ s^{-1}\ m_t^{-3}$) and the zero value related to full tissue coagulation. Moreover, as the perfusion coefficient increases, a departure from the standard curve is now observed. For example, the $\omega_b = 0.02\ m_b^3\ s^{-1}\ m_t^{-3}$ situation, which is typically encountered in the duodenum of dogs (Kapin and Ferguson, 1985), presents a 3.5 % deviation from the curve related to the second case of Table 2. Also worth mentioning is the fact that with the increase of life expectancy, the frequency of tumors in the digestive system becomes more recurrent. If one envisions the situation in which malignant cells are present in the duodenum, a case associated to a much higher perfusion coefficient, here taken as $\omega_b = 0.2\ m_b^3\ s^{-1}\ m_t^{-3}$, a noticeable 22% fluctuation

is computed. This behavior is consistent with the role of the perfusion term in the Pennes equation. For this particular treatment, the perfusion term behaves as a sink term and accordingly, an increased value of $\omega_b$ yields to lower profiles of the temperature distribution.

| Case | $\omega_b$ [$m_b^3 s^{-1} m_t^{-3}$] |
|---|---|
| *1* | 0 |
| *2* | 0.0005 |
| *3* | 0.02 |
| *4* | 0.2 |

Table 2: Blood perfusion values used in the simulations.

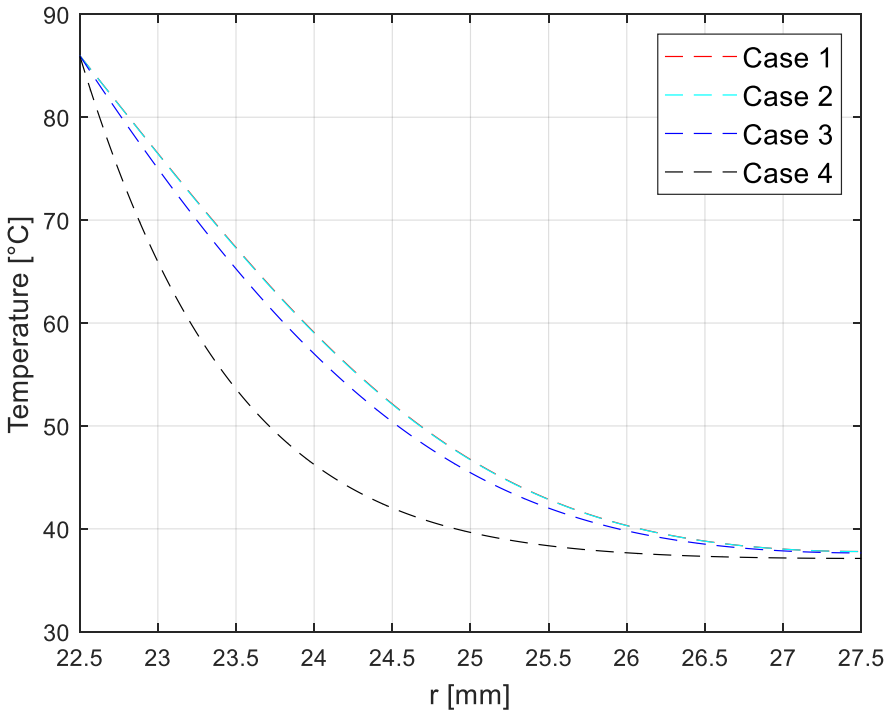


Figure 3: Temperature distribution at $t$ = 10 s for distinct values of blood perfusion.

In an attempt to analyze the irreversible thermal damage caused by the proposed heating therapy, the Arrhenius model described at Eq. (6) was used considering typical values associated to tissue ablation (Fugitt, 1955; Ye and De, 2017). A frequency factor ($A$) of $5 \times 10^{45}$ $s^{-1}$ and a value of $2.96 \times 10^5$ J $mol^{-1}$ to the activation energy ($E_a$) were utilized while the universal gas constant was taken as 8.314 J $mol^{-1}K^{-1}$. The degree of the tissue damage is illustrated in Figure 4 and a distinct three-layer pattern is observed for each of the simulated perfusion coefficients. The top layer refers to a region of the duodenum which is not thermally affected by the procedure. In other words, during the whole extent of the 10 s treatment the temperature is consistently below 42 °C and the computed value of the Henriques integral is under unity. The middle layer is a region where the temperature reaches at least 42 °C at some point of the treatment but $\Omega < 1$ and therefore the biological tissue is capable of full regeneration. The bottom layer is the one in which an irreversible biological damage is induced by the procedure as $\Omega \geq 1$.

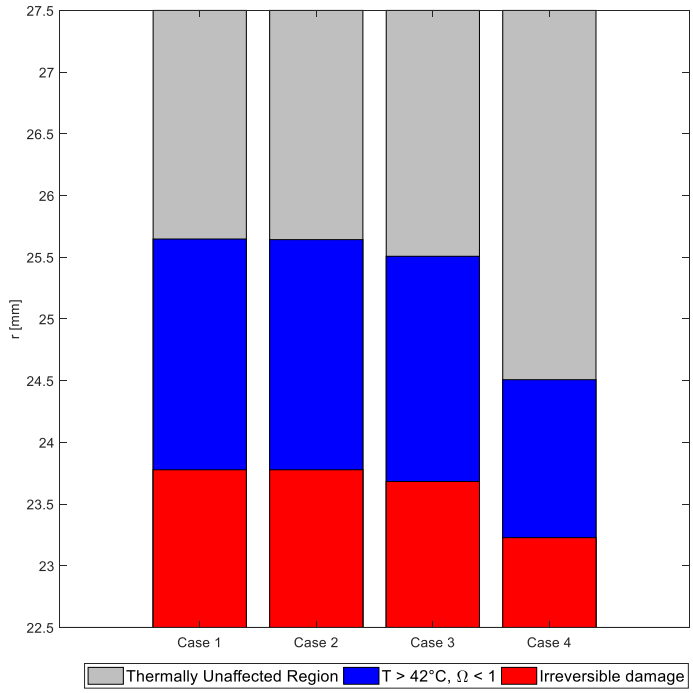


Figure 4: Region affected by the treatment.

From a numerical perspective, the simulations indicate that for the first and second cases of Table 2, the irreversible thermal damage is around 1.3 mm and is only about 0.7 mm for the higher value of the perfusion coefficient. The region susceptible to full regeneration is about 3.1 mm for the expected values of a healthy human but reduces to only 2.0 mm for the case with higher value of the perfusion coefficient.

The unaffected region lies between the range of the 1.9 to 3.0 mm of the latter portion of the duodenum depending on the value of the perfusion blood rate. As a final note, the metabolic heat rate does not appear to play a major role in the thermal problem as numerical simulations for different values of that of Table 1 did not produce significant deviations from the results in the above analysis.

## 5 CONCLUSIONS

This research attempted to perform a numerical analysis of the Duodenal Mucosal Resurfacing treatment for Type 2 diabetes. The main purpose of this work was to evaluate the temperature distribution along the duodenum wall and determine the value of the Henriques integral for the 10 s procedure. Both the FEM and the FVM were successfully employed in the solution of the Pennes bioheat transfer equation as they yielded extremely similar results. In brief, the simulations reported in this contribution suggest that the extent of the affected region is strongly dependent on the blood perfusion rate of the duodenum. More specifically, the region capable of producing new cells which are more efficient in sending a signal to the pancreas for the appropriate level of insulin production lies in the range of 40 % to 62 % of the duodenum wall.

## REFERENCES

Abraham, J.P., Nelson-Cheeseman, B.B., Sparrow, E., Wentz, J.E., Gorman, J.M., and Wolf, S.E., Comprehensive method to predict and quantify scald burns from beverage spills. *International Journal of Hyperthermia*, 32:900-910, 2016.

Abraham, J.P., Plourde, B.D., Vallez, L.J., Nelson-Cheeseman, B.B., Stark, J.R., Sparrow, E.M., and Gorman, J.M, Skin burns. In Shrivastava, D. (Ed.), *Theory and Applications of Heat Transfer in Humans*, John Wiley & Sons Ltd, Chapter 33:723-739, 2018.

ASME, *Standard for verification and validation in computational fluid dynamics and heat transfer*. The American Society of Mechanical Engineers, ASME V&V 20- 2009.

Frøkjær, J.B., Andersen, S.D., Drewes, A.M., and Gregersen, H., Ultrasound-determined geometric and biomechanical properties of the human duodenum. *Digestive Diseases and Sciences*, 51:1662–1669, 2006.

Fugitt, C.E., A rate process of thermal injury. *Armed Forces Special Weapons Project AFSWP*-606, 1955.

Hadefi, A., Huberty, V., Lemmers, A., Arvanitakis, M., Maggs, D., Costamagna, G., and Devière, J., Endoscopic duodenal mucosal resurfacing for the treatment of type 2 diabetes. *Digestive Diseases*, 36(4):322-324, 2018.

Henriques, F.C. Jr., Studies of thermal injury V. The predictability and the significance of thermally induced rate processes leading to irreversible epidermal injury. *Archives of Pathology*, 43(5):489-502, 1947.

Henriques, F.C. Jr., and Moritz, A.R., Studies of thermal injury I. The conduction of heat to and through skin and the temperatures attained therein: A theoretical and an experimental investigation. *American Journal of Pathology*, 23(4):531-549, 1947.

Kapin, M.A., and J.L. Ferguson., Hemodynamic and regional circulatory alterations in dog during anaphylactic challenge. *American Journal of Pathology*, 249(2):H430-H437, 1985.

Moritz, A.R., Studies of thermal injury III. The pathology and pathogenesis of cutaneous burns: an experimental study. *American Journal of Pathology*, 23(6):915-941, 1947.

Moritz, A.R., and Henriques, F.C. Jr., Studies of thermal injury II. The relative importance of time and surface temperature in the causation of cutaneous burns. *American Journal of Pathology*, 23(5):695-720, 1947.

Ozisik, M.N., Orlande, H.R.B., Colaço, M.J., and Cotta, R.M., *Finite Difference Methods in Heat Transfer*. Boca Raton: CRC Press, 2nd edition, 2017.

Patankar, S.V., *Numerical heat transfer and fluid flow*. Hemisphere Publishing Corporation, 1980.

Pearce, J.A., Comparative analysis of mathematical models of cell death and thermal damage process, *International Journal of Hyperthermia*, 29(4): 262–280, 2013.

Pennes, H.H., Analysis of tissue and arterial blood temperatures in the resting human forearm. *Journal of Applied Physiology*, 1(2):93-122, 1948.

Rajagopalan, H., Cherrington, A.D., Thompson C.C., Kaplan, L.M., Rubino, F., Mingrone, G., Becerra, P., Rodriguez, P., Vignolo, P., Caplan, J., Rodriguez, L., and Neto, M.P.G., Endoscopic duodenal mucosal resurfacing for the treatment of type 2 diabetes: 6-month interim analysis from the first-in-human proof-of-concept study. *Diabetes Care*, 39:2254–2261, 2016.

Rossmann, C., and Haemmerich, D., Review of temperature dependence of thermal properties, dielectric properties, and perfusion of biological tissues at hyperthermic and ablation temperatures. *Critical Review Biomedical Engineering*, 42(6): 467–492, 2014.

Thomsen, S.L., and Pearce, J.A., Thermal damage and rate processes in biological tissues. In

Welch, A.J., and van Gemert, M.J.C. (Eds.), *Optical-Thermal Response of Laser-Irradiated Tissue*, 2nd ed., chap. 13, Springer Science+Business Media B.V., 2011.

Valvano, J.W., Thermal property measurements. In Shrivastava, D. (Ed.), *Theory and Applications of Heat Transfer in Humans,* 17: 333-354, John Wiley & Sons Ltd, 2018.

Valvano, J.W., Tissue thermal properties and perfusion. In Welch, A.J., and van Gemert, M.J.C. (Eds.), *Optical-Thermal Response of Laser Irradiated-Tissue*, 12:455-486, Springer, 2nd edition, 2011.

Wright, N.T., Quantitative models of thermal damage to cells and tissues. In Becker, S.M., and Kuznetsov, A.V. (Eds.), *Heat Transfer and Fluid Flow in Biological Processes*, Chap. 3, Elsevier, 2015.

Ye, H., and De, S., Thermal injury of skin and subcutaneous tissues: A review of experimental approaches and numerical models. *Burns*, 43(5): 909–932, 2017.

Zhao, G., Panhwar, F., and Chen, Z., Modeling combined cryosurgery and hyperthermia with thermally significant blood vessels. In Shrivastava, D. (Ed.), *Theory and Applications of Heat Transfer in Humans*, John Wiley & Sons Ltd, Chapter 30:669-685, 2018.